



This is a repository copy of *Anatomical constraints to C4 evolution: light harvesting capacity in the bundle sheath.*

White Rose Research Online URL for this paper:
<http://eprints.whiterose.ac.uk/102240/>

Version: Accepted Version

Article:

Bellasio, C. and Lundgren, M.R. (2016) Anatomical constraints to C4 evolution: light harvesting capacity in the bundle sheath. *New Phytologist*, 212 (2). pp. 485-496. ISSN 0028-646X

<https://doi.org/10.1111/nph.14063>

"This is the peer reviewed version of the following article: Anatomical constraints to C4 evolution: light harvesting capacity in the bundle sheath, which has been published in final form at <http://dx.doi.org/10.1111/nph.14063>. This article may be used for non-commercial purposes in accordance with Wiley Terms and Conditions for Self-Archiving.

Reuse

Unless indicated otherwise, fulltext items are protected by copyright with all rights reserved. The copyright exception in section 29 of the Copyright, Designs and Patents Act 1988 allows the making of a single copy solely for the purpose of non-commercial research or private study within the limits of fair dealing. The publisher or other rights-holder may allow further reproduction and re-use of this version - refer to the White Rose Research Online record for this item. Where records identify the publisher as the copyright holder, users can verify any specific terms of use on the publisher's website.

Takedown

If you consider content in White Rose Research Online to be in breach of UK law, please notify us by emailing eprints@whiterose.ac.uk including the URL of the record and the reason for the withdrawal request.



eprints@whiterose.ac.uk
<https://eprints.whiterose.ac.uk/>

Anatomical constraints to C₄ evolution: light harvesting capacity in the bundle sheath

Chandra Bellasio and Marjorie R. Lundgren

Department of Animal and Plant Sciences, University of Sheffield, Sheffield, S10 2TN, UK

Correspondence: c.bellasio@sheffield.ac.uk, +44 (0) 114 2220093

Keywords

bioengineering, bundle sheath extension, C₃–C₄, crops, light penetration, light profiles, Poaceae, grasses

Running title

Light harvesting in bundle sheaths

Total word count (excluding summary, references and legends):	5505	No. of figures:	4
Summary:	199	No. of Tables:	2
Introduction:	678	No of Supporting Information files:	3
Materials and Methods:	1501		
Results:	1362		
Discussion:	1867		
Acknowledgements:	118		

Summary

- In C_4 photosynthesis CO_2 assimilation and reduction are typically coordinated across mesophyll (M) and bundle sheath (BS) cells, respectively. This system consequently requires sufficient light to reach BS to generate enough ATP to allow RuBP regeneration in BS. Leaf anatomy influences BS light penetration and therefore constrains C_4 cycle functionality.
- Using an absorption scattering model (coded in Excel, and freely downloadable) we simulate light penetration profiles and rate of ATP production in BS across the C_3 , C_3 – C_4 , and C_4 anatomical continua.
- We present a trade-off for light absorption between BS pigment concentration and space allocation. C_3 BS anatomy limits light absorption and benefits little from high pigment concentrations. Unpigmented BS extensions increase BS light penetration. C_4 and C_3 – C_4 anatomies have the potential to generate sufficient ATP in the BS, while typical C_3 anatomy does not, except some C_3 taxa closely related to C_4 groups.
- Insufficient volume of BS, relative to M, will hamper a C_4 cycle via insufficient BS light absorption. Thus, BS ATP production and RuBP regeneration, coupled with increased BS investments, allow greater operational plasticity. We propose that larger BS in C_3 lineages may be co-opted for C_3 – C_4 and C_4 biochemistry requirements.

Introduction

The high yield potential of the C₄ photosynthetic pathway has attracted considerable attention, with significant resources being allocated toward engineering C₄-like carbon concentrating mechanisms into C₃ crops (c4rice.irri.org, www.3to4.org) (Sheehy, 2007; Hibberd et al., 2008; Gowik & Westhoff, 2011). In natural systems, evolution of C₄ photosynthesis entails modifications to the typical ancestral C₃ anatomy. In particular, the bundle sheath (either inner or outer, see Fig. 1, collectively referred to as BS, abbreviations are listed in Table 1) total area increases relative to mesophyll (M) to accommodate the photosynthetic machinery required in the BS (Hattersley, 1984; Dengler et al., 1994; Dengler & Nelson, 1999; Sage, 2004) and, in some species, becomes partially isolated from the surrounding M by deposition of a gas-tight cell wall (von Caemmerer & Furbank, 2003). The anatomical modifications at the BS / M interface and the genetic implications of the biochemical compartmentalisation of the BS have been comprehensively studied (Kajala et al., 2011; von Caemmerer et al., 2012; Lundgren et al., 2014), however, little attention has been paid to energetics.

Unlike the C₃ pathway, C₄ photosynthesis demands substantial amounts of ATP in the BS for the regeneration of glycolate and Ribulose-1,5-bisphosphate (RuBP) (Kanai & Edwards, 1999), which presents a well-defined threshold required to operate a fully engaged C₄ system (Bellasio & Griffiths, 2014c). When insufficient ATP is generated in the BS, the C₄ system is disrupted and may lead to stunted growth and other adverse phenotypes, such as chlorosis and decreased carbohydrate content (McQualter et al., 2016). Because ATP is not a diffusible metabolite, ATP demand in the BS has to be met by a functional electron transport chain (Driever & Kromdijk, 2013), driven by sufficient light reaching the BS (Evans et al., 2007; Kramer & Evans, 2011; Bellasio & Griffiths, 2014c). The concentric anatomy of grass leaves, characterized by vascular bundles encircled by BS and radiate M layers (Fig.1a), has a critical role in determining the light harvesting potential of BS (Evans et al., 2007; Bellasio & Griffiths, 2014c). For instance, the thickness and density of the light harvesting machinery (hereafter pigmentation) of adaxial mesophyll (MAD) and abaxial mesophyll (MAB, collectively referred to as MA hereafter) will influence the ability of light to reach the BS, as they effectively shade it. However, this shading may be reduced by the presence of unpigmented extraxylary fibres and bundle sheath extensions (collectively referred to as BSE hereafter) within MAD or MAB (Karabourniotis et al., 2000). Until now, little work has been done to explore the role of BSE in facilitating light penetration of the BS. Despite their

obvious importance, light harvesting and energy constraints across the leaf anatomical continua associated with C₃ to C₄ evolutionary transitions have not been quantified, and there is a timely need for realistic predictions of these factors in the design of manipulative projects.

In this work we hypothesize that the anatomy of grass leaves constrains the operation of C₄ photosynthesis, mediated by light availability and ATP production in the BS. By describing the likely profiles of light penetration in a leaf, an absorption scattering model is used here to calculate the proportion of absorbed light (AB) in BS relative to that absorbed in M, expressed as $AB \frac{BS}{M}$. The model is parameterised with measured anatomical characteristics from a range of C₃, C₃–C₄, and C₄ representatives to study the light harvesting potential across this anatomical gradient in grasses and three hypothetical scenarios are simulated. First, manipulation of the BS pigmentation parameter allows us to quantify the potential for light harvesting in the BS of C₃, C₃–C₄, and C₄ anatomical types. Then, we quantify the optimal proportion of inter-veinal distance (IVD) allocation to BS across several targets of $AB \frac{BS}{M}$, and finally, we explore the effects of manipulating BSE pigmentation on light absorption in the BS. Within this operational framework, we show the influence of various leaf anatomies on potential ATP production (J_{ATP}) in the BS, $\frac{J_{ATP}^{BS}}{J_{ATP}^M}$. We then put these findings into a broader context by applying the model to 145 species from across the grass phylogeny to infer how the relationship between leaf anatomy and energetics may influence the evolution of C₄ photosynthesis.

Materials and Methods

Quantifying leaf anatomy across the C₃ to C₄ continuum

Images of leaves in cross-section were obtained from rice (C₃), wheat (C₃), *Homolepis aturensis* (C₃–C₄), and maize (C₄) plants, as well as C₃ (KWT), C₃–C₄ (L01 and L04), and C₄ (MDG) accessions of *Alloteropsis semialata* [Fig. 1a, Supporting Information Fig. S1, (Christin et al., 2013; Osborne et al., 2014; Lundgren et al., 2016)]. Tissue samples of wheat and *A. semialata* leaves 3–5 mm in length were fixed in 4:1 ethanol:acetic acid, and embedded in methacrylate embedding resin (Technovit 7100, Heraeus Kulzer GmbH, Wehrheim, Germany). Embedded leaves were sectioned between 6–8 μm thick on a manual rotary microtome (Leica Biosystems, Newcastle, UK). The cross-sections of *A. semialata* were stained with Toluidine Blue O and wheat with Safranin O (Sigma-Aldrich, St. Louis, MO, USA). Slides of rice and maize cross-sections were obtained from commercial suppliers

(Griffin Education, Loughborough, UK). All cross-sections were photographed using microscopy imaging software and a camera mounted on a microscope (CellA; Olympus DP71; BX51, respectively. Olympus, Hamburg, Germany). The cross-section image of *H. aturensis* used in Christin et al. (2013) was used here, with permission of the authors.

While all C_3 and C_4 grasses typically have at least three orders of vein size (i.e., the mid-rib or primary vein, followed by secondary veins characterized by having metaxylem, and tertiary veins that lack metaxylem), only C_4 species typically have minor veins of lesser orders [reviewed in (Sack & Scoffoni, 2013); (Lundgren et al., 2016)]. Thus, tertiary veins (e.g., Fig. 1a) were chosen to represent the functional light-harvesting unit in this study, as the primary vein has mainly a support function (Moulia et al., 1994), secondary veins primarily have hydraulic and mechanical functions (Niinemets et al., 2007), while tertiary veins are more abundant than either primary or secondary veins and are present and ontogenetically similar across the three photosynthetic types. Furthermore, the vasculature in tertiary veins is smaller than in secondary veins, which facilitates the successive modelling stage. Tertiary vein anatomy is schematised in Fig. 1b. Anatomical traits were measured using ImageJ v1.49 (Schneider et al., 2012) and averaged across all tertiary veins within a single segment (i.e., a portion of cross-section stretching between two secondary veins), yielding between three and six replicate tertiary veins per accession. IVD was calculated as segment length divided by the total number of veins, including the initial secondary vein, within that segment. The heights and widths of the vein (defined here as the bundle encompassing both vasculature and bundle sheaths) and abaxial and adaxial BSE were measured (vein height, vein width, AB.BSE.H, AD.BSE.H, AB.BSE.W, and AD.BSE.W, respectively, Fig. 1b). The height of the leaf cross-section was measured along the vein (height at vein, Fig. 1b), together with other quantities detailed in Supporting Information Table S3. The vein height and vein width (Fig. 1b) were used to calculate the total vein area as an ellipse ($vein\ area = \pi \frac{1}{2} vein\ height \frac{1}{2} vein\ width$).

To evaluate the pigmentation of M and BS, cross-sections of fresh leaves were cut by hand, mounted with water, then imaged as described above (examples shown in Supporting Information Fig. S2). Tertiary vein RGB images were processed in ImageJ and hand-segmented in regions corresponding to M, vein, and unpigmented areas (BSE plus epidermis) within the leaf profile. The histogram of the RGB channel was extracted for between four and eight replicates per region (full dataset available in Supporting Information Table S3), and the weighted average histogram value (WAV, which is perceived by the human eye as

luminosity of that region) was computed. The apparent relative absorbance (ARA) was calculated as:

$$ARA = \frac{\log_{10} \frac{WAV_{Unpigmented}}{WAV_{Vein}}}{\log_{10} \frac{WAV_{Unpigmented}}{WAV_M}}, \quad 1$$

which, according to the Beer–Lambert Law, represents the ratio of pigment concentration averaged over the vein, relative to M.

A model for light penetration in a leaf

The model presented in Bellasio and Griffiths (2014c) was modified to account for variable geometry and the presence of BSE. The light–absorbing portion of a leaf in cross–section was simulated in rectangular units, enclosing a rectangular vein (Fig. 1c). The rectangular anatomy was functional to simulate the leaf light environment in two distinct light profiles: P1, sectioning the interveinal mesophyll and P2, sectioning the vein, MAD and MAB, respectively (all three assumed to be uniform compartments, Fig. 1c). P1 and P2 were calculated according to the Kubelka–Munk absorption–scattering theory (Kubelka & Munk, 1931; Allen & Richardson, 1968; Gates, 1980) as in Bellasio and Griffiths (2014c). P2 light profiles were discontinuous, as they represented three different compartments: MAD, vein, and MAB. P2 light penetration profiles were calculated using two values of pigmentation (k), one for MAD and MAB, k_{MA} , and one for the vein, k_V . These were related to the interveinal M pigmentation, k_{MI} , by the input parameters $\frac{k_{MA}}{k_{MI}}$ and $\frac{k_V}{k_{MI}}$, physiologically representing MA pigmentation (fraction of MA which is pigmented and not BSE), and the pigmentation of the vein (relative to interveinal M), respectively. Profiles were integrated, fitted and put into leaf–level context by weighing the fractions of IVD represented by P1 and P2 thus resulting in light absorbed in BS, relative to M $\left(AB \frac{BS}{M} \right)$. Model details are reported in Supporting Information Method S1 and Note S2. The possible sources of error, and a comparison with other modelling approaches are reported in Supporting Information Note S3.

Empirical parameterisation

The complex and diverse anatomical traits needed to be standardised to be inputted to the optical model. Unpigmented epidermis was neglected. Height at vein was set to correspond to

$N=1000$ layers. The heights of MAD and MAB (AD.BSE.H and AB.BSE.H) were expressed as a fraction of N , as number of layers n_{MAD} and n_{MAB} , respectively. The vein equivalent height (VEH) was calculated as: $VEH = height\ at\ vein - AD.BSE.H - AB.BSE.H$, and also inputted as number of layers n_{VEIN} (where $N=n_{MAD}+n_{VEIN}+n_{MAB}$). The vein equivalent width (VEW) was calculated as: $VEW = \frac{vein\ area}{VEH}$, to preserve the ratio between vein area and total section area ($IVD \times height\ at\ vein$). The ratio between vein equivalent width and interveinal distance, $\frac{VEW}{IVD}$, was taken as the fraction of IVD represented by P2. The average fraction of MAB and MAB not occupied by BSE $\left(1 - \frac{AD.BSE.W+AB.BSE.W}{2VEW}\right)$ was taken as the relative MA pigmentation $\frac{k_{MA}}{k_{MI}}$. ARA was taken as $\frac{k_V}{k_{MI}}$.

From light harvesting to ATP production

The ATP production rate in BS ($J_{ATP\ BS}$), relative to ATP production rate in M ($J_{ATP\ M}$), can be written as:

$$\frac{J_{ATP\ BS}}{J_{ATP\ M}} \approx \left(1 + r_{AB_{CEF\ BS}} \left(\frac{\eta_{CEF\ BS}}{\eta_{LEF\ BS}} - 1\right)\right) AB \frac{BS}{M}, \quad 2$$

where $r_{AB_{CEF\ BS}}$ is the fraction of AB_{BS} used by cyclic electron flow (CEF), and η_{CEFBS} and η_{LEFBS} are the overall conversion yield of AB_{BS} in J_{ATP} of CEF and linear electron flow (LEF), respectively (full derivation is included in Supporting Information File S1 Note 4). η_{CEFBS} and η_{LEFBS} depend on many physical and physiological factors, some of which are very difficult to measure and remain debated (Yin et al., 2004; Yin & Struik, 2012). The electron transport chain model presented by (Yin et al., 2004) was shown to be applicable along the C_3 to C_4 continuum (Yin et al., 2011; Yin & Struik, 2012; Yin & Struik, 2015). The model was modified (Bellasio, unpublished) to account for the possibility of CEF mediated by the NDH complex (Kramer & Evans, 2011; Peng et al., 2011), which is essential for C_4 photosynthesis (Nakamura et al., 2013; Yamori & Shikanai, 2016). $\frac{\eta_{CEF\ BS}}{\eta_{LEF\ BS}}$ can be estimated at c. 2 when the initial yield of PSI and PSII (extrapolated under zero PPF) are 1 and 0.8, respectively, additional electron sinks are considered negligible, the quinone cycle is assumed to be obligate, the NDH-mediated electron flow, and the PGR5 / PGRL1-mediated electron flow (Kramer & Evans, 2011; Peng et al., 2011; Hertle et al., 2013), both operating in BS (Ivanov et al., 2007), are equally weighed. The stoichiometry of the ATP synthase was mathematically simplified to be the same as the phosphorylating enzyme complex (Majeran

& van Wijk, 2009; Friso et al., 2010). Furthermore, $r_{AB_{CEF_{BS}}}$ was not measured directly because the M and BS signals cannot be deconvoluted through spectroscopy, so we calculated Eqn 2 at any possible $r_{AB_{CEF_{BS}}}$ value. To give a broad idea of the operational conditions, however, we used a generalised stoichiometric model of assimilation (Bellasio, under review) to estimate the NADP and ATP requirements for C_3 and C_4 photosynthesis, and coupled that with the aforementioned electron transport chain model. For a C_4 plant, Rubisco specificity is 2400, the ratio between ATP and NADPH demand would be 2.77, and the required $r_{AB_{CEF_{BS}}}$ would be c. 0.85 when $AB_{\frac{BS}{M}}$ is c. 0.65, under saturating light and with a CO_2 concentration at the carboxylating sites of $250 \mu\text{mol mol}^{-1}$. Similar considerations can be made for M chloroplasts in C_3 plants. The ratio between ATP and NADPH demand would be 1.62, and the required $r_{AB_{CEF_{BS}}}$ would be c. 0.1. Because we are interested in the potential $\frac{J_{ATP_{BS}}}{J_{ATP_M}}$ here, we hypothesized that plants could acclimate $r_{AB_{CEF_{BS}}}$ through state transition and electron transport chain adjustments, and reach a maximal $r_{AB_{CEF_{BS}}}$ of 1 and 0.375, for C_4 plants and C_3 plants, respectively, and an intermediate value of 0.7 for C_3 - C_4 taxa.

Results

The C_3 to C_4 anatomical continuum

The study accessions presented a wide range of anatomical variation typical of that observed across the C_3 to C_4 gradient in grasses (Lundgren et al., 2014). The IVD was largest in C_3 ($\geq 255 \mu\text{m}$), and smallest in C_4 ($< 125 \mu\text{m}$), types with C_3 - C_4 accessions presenting IVD between that of C_3 and C_4 accessions (195–207 μm ; Table 2, Supporting Information Table S3). The proportion of IVD composed of vein (VEW/IVD) was smallest in rice and wheat, largest in the two C_4 accessions, and intermediate in the three C_3 - C_4 accessions and C_3 *A. semialata* (Table 2). The number and size of tertiary veins and leaf height at these veins did not differ by photosynthetic type (Table 2, Supporting Information Table S3). The tertiary veins of all accessions except wheat had $BSE \left(\frac{k_{MA}}{k_{MI}} < 1 \right)$. These were largest in maize and the C_3 - C_4 and C_4 *A. semialata* accessions and smallest in rice and *H. aturensis*. The accessions had variable pigmentations of the BS relative to M (ARA). While rice had very little to no BS pigmentation, wheat had about one-tenth, and the C_3 and C_3 - C_4 *A. semialata* accessions approximately one-third, the ARA of maize (Table 2, Supporting Information Table S3). The C_4 *A. semialata* had over one and a half times the ARA of maize.

Using the measured anatomical traits, a first set of model outputs generated $AB \frac{BS}{M}$, which revealed clear differences between photosynthetic types in their ability to absorb light and produce J_{ATP} in BS. Rice and wheat harvested negligible amounts of light in BS ($AB \frac{BS}{M}=0.001$ and 0.03 , respectively; Table 2), while maize harvested 40% ($AB \frac{BS}{M}=0.66$) and C_4 *A. semialata* as much as 61% ($AB \frac{BS}{M}=1.6$) of light in the BS. $AB \frac{BS}{M}$ in the C_3 – C_4 individuals were intermediate between those calculated for C_3 and C_4 accessions. When the operational $\frac{J_{ATP BS}}{J_{ATP M}}$ was calculated using likely values for $rAB_{CEF BS}$ (Table 2), rice and wheat generated a negligible amount of ATP in BS ($\frac{J_{ATP BS}}{J_{ATP M}}=0.001$ and 0.04 , respectively), while maize and C_4 *A. semialata* produced the most ($\frac{J_{ATP BS}}{J_{ATP M}}=1.32$ and 3.21 , respectively), and C_3 – C_4 accessions intermediate amounts of ATP in the BS (Table 2). The C_3 *A. semialata* had $AB \frac{BS}{M}$ and $\frac{J_{ATP BS}}{J_{ATP M}}$ intermediate between the other C_3 accessions and the C_3 – C_4 taxa (Table 2).

A second set of model outputs was generated by selectively varying vein pigmentation, vein size, the size of BSE, and the engagement of CEF in BS, as described below. These scenarios are useful to investigate the potential for light harvesting and ATP production in BS, in the hypothetical case that operational values could be manipulated, to highlight the possible bottlenecks and preferred routes to bio–engineering.

How much light could potentially be absorbed in the BS if we could freely manipulate BS pigmentation?

This simulation explored the potential for increasing $AB \frac{BS}{M}$ by manipulating BS pigmentation without modifying leaf anatomy. The model was parameterised with the anatomical characteristics (as n_{MAD} , n_{VEIN} , n_{MAB} , VEW/IVD , and $\frac{k_{MA}}{k_{MI}}$) of six accessions (Table 2), and $AB \frac{BS}{M}$ was calculated at different levels of vein pigmentation ($\frac{k_V}{k_{MI}}$). The model output indicates a clear differentiation between C_3 , C_4 and intermediate types (Fig. 2a). For example, when $\frac{k_V}{k_{MI}}=1$ the BS of C_3 plants absorb only about a fifth, and C_3 – C_4 types just over a half, of that absorbed in maize BS. Moreover, C_3 types show a quasi–saturation when $\frac{k_V}{k_{MI}}>1$, suggesting that plants with typical C_3 anatomy would benefit little from increasing BS pigment concentration further. Absorbed light in the BS of C_4 and C_3 – C_4 plants, however,

continues to increase up to $\frac{k_V}{k_{MI}}=3$. While the two C₃ accessions presented very similar responses of $AB \frac{BS}{M}$ to increasing $\frac{k_V}{k_{MI}}$, as did the two C₃–C₄ plants, the two C₄ accessions differed in this relationship, with *A. semialata* MDG reaching twice the $AB \frac{BS}{M}$ as maize when $\frac{k_V}{k_{MI}}=3$ (Fig. 2a).

How much space needs to be committed to veins to harvest a target $AB \frac{BS}{M}$?

In this simulation, relative vein size (as VEW/IVD) and pigmentation ($\frac{k_V}{k_{MI}}$) were varied, while the number of layers attributed to MAD, vein, and MAB (n_{MAD} , n_{VEIN} , n_{MAB}), and MA pigmentation ($\frac{k_{MA}}{k_{MI}}$) were set to those of the average leaf anatomy across six study accessions (Table 2). Practically, $\frac{k_V}{k_{MI}}$ was increased in steps from 0.1 to 3 and VEW/IVD was iteratively fitted until a target value of $AB \frac{BS}{M}$ was reached. Fig. 2b shows a trade-off between pigmentation and vein size. In other words, the same fraction of incident light can be harvested (e.g., $AB \frac{BS}{M}=1.0$) either by small dark (VEW/IVD = 0.5; $\frac{k_V}{k_{MI}} = 3.0$) or large pale (VEW/IVD=0.8; $\frac{k_V}{k_{MI}} = 0.5$) veins, within a certain window of plasticity.

What is the effect of BSE on $AB \frac{BS}{M}$?

The effect of BSE size was simulated by manipulating MA pigmentation $\frac{k_{MA}}{k_{MI}}$, using the anatomical constraints (n_{MAD} , n_{VEIN} , n_{MAB} , and VEW/IVD) averaged across six accessions (Table 2). Testing three levels of vein pigmentation ($\frac{k_V}{k_{MI}} = 0.5, 1, 2$), we show that the presence and size of BSE considerably increases light absorption in the BS. Moreover, the proportional increase in $AB \frac{BS}{M}$ was greater when vein pigmentation was low than when it was high (73% versus 45% in $\frac{k_V}{k_{MI}}=0.5$ and 2.0, respectively; Fig. 2c). For example, if one were to engineer BSE onto the tertiary veins of wheat, given its current relative BS pigmentation (ARA = 0.198), $AB \frac{BS}{M}$ could increase from 0.026 to 0.061 (+134%), however, this would require space to accommodate BSE and would still not be sufficient to sustain ATP demands required for C₄ photosynthesis.

What is the potential for ATP generation in the BS?

To overcome possible uncertainties associated with quantifying the fraction of light used by CEF in the BS ($r_{AB_{CEF\ BS}}$), in this simulation we hypothesized that plants could freely vary $r_{AB_{CEF\ BS}}$ between 0 and 1. This shows the entire range of possible values of $\frac{J_{ATP\ BS}}{J_{ATP\ M}}$ given the measured anatomical constraints. $AB \frac{BS}{M}$ was calculated using the anatomical constraints (n_{MAD} , n_{VEIN} , n_{MAB} , VEW/IVD , and $\frac{k_{MA}}{k_{MI}}$) averaged across six accessions (Table 2) in a hypothetical case where vein pigmentation is identical across vein and M tissue, $\frac{k_V}{k_{MI}}=1$. The threshold $\frac{J_{ATP\ BS}}{J_{ATP\ M}}=0.3$ required to operate the C_4 pathway (Bellasio & Griffiths, 2014c) is plotted in Fig. 2d as a bold line. C_4 plants exceed the $\frac{J_{ATP\ BS}}{J_{ATP\ M}}$ threshold regardless of $f_{cyc\ BS}$. C_3 – C_4 plants have the potential to sustain the C_4 pathway, but operate close to the threshold, a condition that may result in low operational plasticity (see Discussion). Rice and wheat, however, do not have the potential to regenerate RuBP in BS, regardless of $f_{cyc\ BS}$, due to their low BS to M ratios.

Light harvesting constraints to C_4 evolution

To understand how anatomical constraints to light harvesting may have influenced the ability for C_4 photosynthesis to evolve in grasses, we applied our modelling approach to a dataset of 145 phylogenetically diverse grass species, as presented in Christin et al. (2013). This dataset included 50 C_4 and 61 C_3 species from the PACMAD clade (after Panicoideae, Aristidoideae, Chloridoideae, Micrairoideae, Arundinoideae, Danthonioideae) and 34 C_3 species from the BEP clade (after Bambusoideae, Ehrhartoideae, Pooideae), which never evolved the C_4 pathway. As we were unable to measure pigmentation, ARA was estimated using the correlation presented in Fig. 3. To account for the variability in anatomical traits, we modified the routine for translating raw data into model inputs (see Supporting Information File S1, Note 2). One-way ANOVA, followed by post-hoc Tukey tests, found that C_4 species have greater VEW/IVD than C_3 grasses (Fig. 4a). Moreover, C_3 species from the PACMAD clade had greater VEW/IVD than those from the BEP clade. C_4 species had greater $AB \frac{BS}{M}$, and thus higher $\frac{J_{ATP\ BS}}{J_{ATP\ M}}$, than C_3 species from both PACMAD and BEP clades (Fig. 4b and 4c). Although $\frac{J_{ATP\ BS}}{J_{ATP\ M}}$ was below the 0.3 threshold necessary to operate the C_4 pathway in C_3 species as a whole, six C_3 species from the PACMAD clade exceeded this threshold (Supporting Information Table S3). These six species belong to the Aristidoideae

(*Sartidia jucunda*) and Panicoideae (*Lecomtella madagascariensis*, *Otachyrium versicolor*, *Hymenachne amplexicaulis*, *Homopholis belsonii*, *Stephostachys mertensii*) subfamilies. Five of these six species are sister to C₄ lineages, while *L. madagascariensis* is not [(Christin et al., 2013); Supporting Information Table S3).

Discussion

Functional links between anatomy and biochemistry

The link between leaf anatomy and photosynthetic type has been well characterized [e.g., (El-Sharkawy & Hesketh, 1965; Laetsch, 1974; Ku et al., 1983; Dengler et al., 1994; Lundgren et al., 2014)], however, the influence of leaf anatomy on the ability for light to penetrate the BS, and consequently generate sufficient ATP to regenerate RuBP (Bellasio & Griffiths, 2014c), has been overlooked despite being a critical factor in C₄ functionality (Bellasio & Griffiths, 2014c; McQualter et al., 2016). Here, we point to the amount of ATP available through photophosphorylation in the BS as a critical bottleneck in the establishment of a functional C₄ cycle, and therefore we link leaf anatomy, and its influence on light harvesting in BS, to biochemical traits.

The relatively small BS of typical C₃ species do not permit a C₄ cycle to function, regardless of pigment concentration. In rice, for instance, even a 100-fold increase in the relative pigmentation of BS (ARA=0.0033, currently), given its current BS size (VEW/IVD = 0.134, currently), would still yield insufficient BS light absorption ($AB \frac{BS}{M} = 0.04$) to surpass the minimum threshold (c. $AB \frac{BS}{M} = 0.15$) needed to regenerate enough RuBP in BS to operate C₄ photosynthesis [Fig. 2b; Table 2; (Bellasio & Griffiths, 2014c)]. Thus, engineering a C₄ carbon concentrating mechanism (CCM) in a C₃ crop, provided chloroplast physiology and metabolite trafficking were adequate, would require increasing the relative proportion of BS to M tissue, whether by decreasing M cell size or number, decreasing leaf thickness, increasing the size of BS cells, or increasing the number of vein units by inserting minor veins or distinctive cells [reviewed in (Lundgren et al., 2014)].

The C₄ plants maize and *A. semialata* MDG exceed the threshold needed to run C₄ photosynthesis by a considerable safety margin, which is likely to counter suboptimal environmental conditions. C₃–C₄ plants have the potential to meet the requirements for a fully engaged C₄ system (i.e., exceed the $\frac{J_{ATP\ BS}}{J_{ATP\ M}}$ threshold), but this can only be achieved by operating substantial amounts of CEF in the BS. The anatomy of the C₃ *A. semialata*

accession can also generate sufficient ATP in the BS to run C₄ photosynthesis ($AB \frac{BS}{M}=0.18$), due to its combination of relatively high BS pigmentation (ARA=0.535), large vein size (VEW/IVD=0.246), and reduced MA pigmentation from the presence of BSE. This trend, whereby C₃ individuals that are closely related to C₄ taxa possess anatomy suitable for C₄ functionality, was also revealed in the larger grass family dataset. While C₄ anatomical phenotypes have been demonstrated in C₃ species in the past and linked to C₄ evolvability (Christin et al. 2013; Griffiths et al. 2013), we put these anatomies into a biochemical context to explain the anatomical thresholds in terms of light and energy requirements.

Operational robustness under changing illumination

The operational values for $\frac{J_{ATP\ BS}}{J_{ATP\ M}}$ listed in Table 2 and the simulations shown in Fig. 2 were calculated assuming that the incident radiation was weakly absorbed (Bellasio & Griffiths, 2014c). The values therefore represent an ideal condition of theoretical maximum achievable when the illumination of the BS chloroplast is optimal. The difference between the operational $\frac{J_{ATP\ BS}}{J_{ATP\ M}}$ under optimal BS illumination and the minimum threshold for $\frac{J_{ATP\ BS}}{J_{ATP\ M}}$ required by C₄ photosynthesis is a safety margin that can be interpreted as an index of the biochemical robustness that a particular anatomical type would have if it were to operate a fully engaged C₄ pathway. Although C₄ plants showed a remarkable capacity to acclimate to reduced light intensities (Ubierna et al., 2013; Bellasio & Griffiths, 2014b; Bellasio & Griffiths, 2014a; Sage, 2014), less penetrating light qualities (e.g., diffuse skylight) will promptly lower $\frac{J_{ATP\ BS}}{J_{ATP\ M}}$. This imposes a reorganisation of assimilatory biochemistry to regulate ATP demand in response to ATP availability (Evans et al., 2007; Sun et al., 2012; Bellasio & Griffiths, 2014c) and while a CCM may still be possible, a fully engaged C₄ system becomes impossible when $\frac{J_{ATP\ BS}}{J_{ATP\ M}}$ falls below the minimum threshold.

This robustness can also be expressed in biochemical terms, by listing the ATP driven metabolic activities that can be supplied in BS under optimal conditions of BS illumination, calculated using the average operational $\frac{J_{ATP\ BS}}{J_{ATP\ M}}$ (Table 2). Typical C₃ grasses do not have the potential to regenerate RuBP in the BS. In contrast, C₃–C₄ plants can supply the totality of Rubisco with RuBP, and regenerate substantial amounts of glycolate, and operate 10% of the reductive pentose phosphate (RPP) cycle in the BS. Maize can supply RuBP to Rubisco, operate 50% of RPP, and 35% of PPK activity in the BS (Aoyagi & Nakamoto, 1985),

which may be engaged to take advantage of transient conditions of ATP availability in the BS (Bellasio & Griffiths, 2014c). *C₄ A. semialata* has a very high operational $\frac{J_{ATP\ BS}}{J_{ATP\ M}}$ of 3.2, which is likely required to supply PEPCK activity in BS, as PEPCK is the prevalent decarboxylating enzyme in this species (Ueno & Sentoku, 2006), (Dunning, et al., unpublished). Because PEPCK activity is required for the CCM to operate it is likely to be modulated in response to assimilatory CO₂ demand in the BS, and cannot concur to fine-tuning ATP demand there (Bellasio & Griffiths, 2014c). In this case the ATP requirements for operating PEPCK would be obligate (the minimum $\frac{J_{ATP\ BS}}{J_{ATP\ M}}$ would therefore increase to c. 1, Bellasio, unpublished). The high $\frac{J_{ATP\ BS}}{J_{ATP\ M}}$ found in *C₄ A. semialata*, consistent with the presence of numerous chloroplasts in the BS (Dengler & Nelson, 1999; Lundgren et al., 2016), may therefore be instrumental to maintain CCM efficiency in conditions of low BS illumination. The isolated BS of some PEPCK plants have shown the capacity, under ATP starvation, to convert malate-derived NADH into ATP through mitochondrial oxidation of NADH (Carnal et al., 1993). This additional flexibility in ATP generation may be a further safety mechanism that PEPCK plants have evolved to overcome the lower biochemical plasticity of the CCM. These findings may help to explain the remarkably broad ecological niche in which *C₄ A. semialata* has come to inhabit (Lundgren et al., 2015).

Economic trade-offs between vein size and pigmentation

When vein size (as $\frac{VEW}{M\ width}$) is plotted against vein pigmentation (as ARA), great variability and, surprisingly, a strikingly linear relationship ($R^2=0.98$; Fig. 3) is found among the six accessions studied. This observation can be explained using economic theory (Hadar, 1966). The two resources ‘size’ and ‘pigmentation’ have a finite cost, which can be evaluated by comparison (e.g., in terms of carbon, nitrogen, or ATP) (Bloom et al., 1985). We show that ‘size’ and ‘pigmentation’ can be co-opted to harvest a target $AB \frac{BS}{M}$ in infinite possible combinations, represented by the curves in Fig. 2b, called ‘isoquants’ in Economics. However, of all possible combinations, plants only operate those lying on the linear relationship plotted in Fig. 3, which is the most efficient combination of ‘size’ and ‘pigmentation’. The line does not pass from the origin (i.e., unpigmented veins have a finite size), as represented here by the rice operational point. Both the intercept and the slope of the line of optimal resource allocation may differ between ecological niches and could in principle be used to compare the benefits of an unpigmented BS (intercept), and the cost of

‘size’ relative to that of ‘pigmentation’ (slope) across different niches. Interestingly, to increase $AB \frac{BS}{M}$, plants scale their investment in ‘size’ and ‘pigmentation’ along the line of optimal resource allocation (Fig. 3). Other combinations of ‘size’ and ‘pigmentation’ on the same isoquant are less efficient. For instance, a small intensely pigmented vein would be relatively inefficient, as higher $AB \frac{BS}{M}$ could be obtained by allocating the same total resource ‘investment’ proportionally more to ‘size’ and less to ‘pigmentation’.

Role of BSE in C_4 evolution

The benefits of BSE were evaluated by diluting MA pigmentation, which strongly increased light absorption in the BS. Moreover, the benefit of BSE were strongest at the low vein pigmentations that are often characterized in C_3 and C_3 – C_4 species (Crooksto & Moss, 1970; Sage et al., 2014). The presence of BSE in some non- C_4 lineages may permit enough light to reach the BS to supply both the C_2 shuttle and C_4 cycle activity. Indeed, we show that large BSE, even in plants with only moderate BS pigmentation (e.g., $\frac{k_V}{k_{MI}}=0.5$), will transmit enough light to reach the threshold $AB \frac{BS}{M}=0.15$ (see above). It has been proposed that BSE may have initially evolved to improve hydraulics (Buckley et al., 2011), compartmentalize the intercellular gaseous environment across the leaf (Terashima et al., 1988), provide structural support (Zhong et al., 1997), or even increase transmission of photosynthetically active radiation to the deeper mesophyll layers (Karabourniotis et al., 2000). Once BSE establish in C_3 lineages for these reasons, they could then be co-opted in the evolution of C_2 and C_4 cycles to functionally increase light transmission to the BS.

Implication for C_4 evolution and bioengineering

In C_3 species, large BS function to store water, osmolytes, and sugars, repair cavitation, provide mechanical support, refix (photo)respiratory CO_2 , and control xylem, mesophyll and stomatal conductance mediated by ABA signalling [reviewed in (Griffiths et al., 2013)]. Here, we point to additional beneficiary functions of larger BS that have been overlooked so far and may influence the evolution of C_4 photosynthesis. Specifically, larger BS have (1) a greater optical cross section that is indispensable for light harvesting and (2) a larger volume in which the ATP-generating light harvesting machinery and biochemical photosynthetic machinery can be accommodated. Indeed, we show that C_3 PACMAD species have larger relative BS sizes than C_3 BEP species and that, as a whole C_3 species do not have the

potential to harvest enough light to support the BS metabolic activities required for C₄ photosynthesis to operate, yet a few specific C₃ species do possess anatomy capable of supporting a C₄ cycle. Thus, these species likely have the shortest phenotypic gap between non-C₄ and C₄ requirements and, as such, we suggest that they be targeted for initial C₄ CCM bioengineering projects.

Conclusion

We put forward a framework to estimate the potential for light harvesting and ATP production associated with various leaf anatomical phenotypes, and highlight the intertwined nature of anatomical and biochemical traits. By testing hypothetical scenarios we show that, even if it were possible to increase pigmentation in BS indefinitely, BS size would limit the potential for light harvesting and ATP production in BS. These findings have been confirmed by analysing a large dataset of 145 species that encompasses a large variation in anatomical traits. Overall, we provide compelling and diversified evidence to support our hypothesis that leaf anatomy mediates light availability in the BS and, as such, constrains the operation of C₄ photosynthesis. In practical terms, the leaf anatomy of typical C₃ plants limits ATP production in the BS, making it impossible to regenerate enough RuBP to operate a functional RPP cycle in the BS. However, some C₃ and C₃-C₄ taxa exist with anatomical phenotypes capable of operating a functional C₄ cycle and we argue that these should be targeted in C₄ evolution and bioengineering studies.

Acknowledgments

We are grateful to Giovanni Agati for support, Paul Hattersley and Colin Osborne for useful comments, Pascal-Antoine Christin for critical review and for making available the large dataset. We thank Emanuela Samaritani for the mean BSE area measured on the large dataset. We gratefully acknowledge funding of CB through an ERC advanced grant (CDREG, 322998) awarded to David J Beerling, and of MRL through the ERC grant ERC-2014-STG-638333 awarded to Pascal-Antoine Christin. We thank two anonymous reviewers for the constructive comments which contributed to the quality of this paper. We thank Alice Mitchell for generating the wheat cross-sections and Jessica Dunn and Emily Beardon for fresh wheat and rice tissue used for pigment analysis.

The Authors have no conflict of interest.

Contributions: CB and ML conceived of the experiment, analysed results, prepared the figures and wrote the paper. CB wrote and coded the models, and run simulations. ML performed anatomical measurements.

Supporting Information

File S1. Supporting Methods, Notes, and Figures:

Fig. S1 Example cross-sections

Fig. S2 Example of RGB images

Methods S1 A model for light penetration in a leaf

Notes S1 Analytical integration of Eqn S1 and S2 after Gates (1980)

Notes S2 Method to derive model inputs from the dataset of Christin et al (2013)

Notes S3 Possible sources of error and comparison with other approaches

Notes S4 Demonstration of Eqn 2

Table S2. Excel workbook coding the anatomical model.

Table S3. Raw data encompassing anatomical and optical measurements and large dataset encompassing 145 species from Christin et al. (2013).

References

- Allen WA, Richardson AJ. 1968. Interaction of light with a plant canopy. *Journal of the Optical Society of America* **58**(8): 1023-1028.
- Aoyagi K, Nakamoto H. 1985. Pyruvate, Pi dikinase in bundle sheath strands as well as in mesophyll cells in maize leaves. *Plant Physiology* **78**(3): 661-664.
- Bellasio C, Griffiths H. 2014a. Acclimation of C₄ metabolism to low light in mature maize leaves could limit energetic losses during progressive shading in a crop canopy. *Journal of Experimental Botany* **65**(13): 3725-3736.
- Bellasio C, Griffiths H. 2014b. Acclimation to low light by C₄ Maize: implications for bundle sheath leakiness. *Plant Cell and Environment* **37**(5): 1046-1058.
- Bellasio C, Griffiths H. 2014c. The operation of two decarboxylases (NADPME and PEPCK), transamination and partitioning of C₄ metabolic processes between mesophyll and bundle sheath cells allows light capture to be balanced for the maize C₄ pathway. *Plant Physiology* **164**: 466-480.
- Bloom AJ, Chapin FS, III, Mooney HA. 1985. Resource limitation in plants-an economic analogy. *Annual Review of Ecology and Systematics* **16**: 363-392.
- Buckley TN, Sack L, Gilbert ME. 2011. The role of bundle sheath extensions and life form in stomatal responses to leaf water status. *Plant Physiology* **156**(2): 962-973.
- Carnal NW, Agostino A, Hatch MD. 1993. Photosynthesis in Phosphoenolpyruvate Carboxykinase-Type C₄ Plants - Mechanism and Regulation of C₄ acid decarboxylation in bundle-sheath cells. *Archives of Biochemistry and Biophysics* **306**(2): 360-367.
- Christin P-A, Osborne CP, Chatelet DS, Columbus JT, Besnard G, Hodkinson TR, Garrison LM, Vorontsova MS, Edwards EJ. 2013. Anatomical enablers and the evolution of C₄ photosynthesis in grasses. *Proceedings of the National Academy of Sciences* **110**(4): 1381-1386.
- Crooksto RK, Moss DN. 1970. Relation of carbon dioxide compensation and chlorenchymatous vascular bundle sheaths in leaves of dicots. *Plant Physiology* **46**(4): 564-567.
- Dengler NG, Dengler RE, Donnelly PM, Hattersley PW. 1994. Quantitative leaf anatomy of C₃ and C₄ Grasses (Poaceae) - Bundle-Sheath and Mesophyll surface-area relationships. *Annals of Botany* **73**(3): 241-255.
- Dengler NG, Nelson T 1999. Leaf structure and development in C₄ plants. In: Sage RF, Monson RK eds. C₄ plant biology. San Diego: Academic Press, 133-172.
- Driever SM, Kromdijk J. 2013. Will C₃ crops enhanced with the C₄ CO₂-concentrating mechanism live up to their full potential (yield)? *Journal of Experimental Botany* **64**(13): 3925-3935.
- El-Sharkawy M, Hesketh J. 1965. Photosynthesis among species in relation to characteristics of leaf anatomy and CO₂ diffusion resistances. *Crop Science* **5**(1): 517-552.
- Evans JR, von Caemmerer S, Vogelmann TC 2007. Balancing light capture with distributed metabolic demand during C₄ photosynthesis. In: Sheehy JE, Mitchell PL, Hardy B eds. Charting new pathways to C₄ rice. Los Baños, Philippines: IRRI International Rice Research Institute.
- Friso G, Majeran W, Huang MS, Sun Q, van Wijk KJ. 2010. Reconstruction of metabolic pathways, protein expression, and homeostasis machineries across maize bundle sheath and mesophyll chloroplasts: large-scale quantitative proteomics using the first maize genome assembly. *Plant Physiology* **152**(3): 1219-1250.
- Gates DM. 1980. *Biophysical Ecology*. New York: Springer Verlag.
- Gowik U, Westhoff P. 2011. The path from C₃ to C₄ Photosynthesis. *Plant Physiology* **155**(1): 56-63.
- Griffiths H, Weller G, Toy LFM, Dennis RJ. 2013. You're so vein: bundle sheath physiology, phylogeny and evolution in C₃ and C₄ plants. *Plant, Cell & Environment* **36**(2): 249-261.
- Hadar J. 1966. *Elementary Theory of Economic Behavior*. Reading, Massachusetts: Addison-Wesley.
- Hattersley PW. 1984. Characterization of C₄ type leaf anatomy in Grasses (Poaceae), Mesophyll - Bundle sheath area ratios. *Annals of Botany* **53**(2): 163-179.
- Hertle AP, Blunder T, Wunder T, Pesaresi P, Pribil M, Armbruster U, Leister D. 2013. PGRL1 is the elusive ferredoxin-plastoquinone reductase in photosynthetic cyclic electron flow. *Molecular Cell* **49**(3): 511-523.
- Hibberd JM, Sheehy JE, Langdale JA. 2008. Using C₄ photosynthesis to increase the yield of rice—rationale and feasibility. *Current Opinion in Plant Biology* **11**(2): 228-231.
- Ivanov B, Asada K, Edwards GE. 2007. Analysis of donors of electrons to photosystem I and cyclic electron flow by redox kinetics of P700 in chloroplasts of isolated bundle sheath strands of maize. *Photosynthesis Research* **92**(1): 65-74.
- Kajala K, Covshoff S, Karki S, Woodfield H, Tolley BJ, Dionora MJA, Mogul RT, Mabilangan AE, Danila FR, Hibberd JM, et al. 2011. Strategies for engineering a two-celled C₄ photosynthetic pathway into rice. *Journal of Experimental Botany* **62**(9): 3001-3010.
- Kanai R, Edwards GE 1999. The biochemistry of C₄ photosynthesis. In: Sage RF, Monson RK eds. C₄ plant biology. San Diego: Academic Press, 49-87.
- Karabourniotis G, Bornman JF, Nikolopoulos D. 2000. A possible optical role of the bundle sheath extensions of the heterobaric leaves of *Vitis vinifera* and *Quercus coccifera*. *Plant, Cell & Environment* **23**(4): 423-430.
- Kramer DM, Evans JR. 2011. The importance of energy balance in improving photosynthetic productivity. *Plant Physiology* **155**(1): 70-78.

- Ku MSB, Monson RK, Littlejohn RO, Nakamoto H, Fisher DB, Edwards GE. 1983.** Photosynthetic characteristics of C₃-C₄ intermediate *Flaveria* species .1. Leaf anatomy, photosynthetic responses to O₂ and CO₂, and activities of key enzymes in the C₃ and C₄ pathways. *Plant Physiology* **71**(4): 944-948.
- Kubelka P, Munk F. 1931.** Ein Beitrag zur Optik der Farbanstriche. *Z Technische Physik*, **12**(S): 593–601.
- Laetsch WM. 1974.** C₄ syndrome - structural-analysis. *Annual Review of Plant Physiology and Plant Molecular Biology* **25**: 27-52.
- Lundgren MR, Besnard G, Ripley BS, Lehmann C, Chatelet DS, Kynast R, Namaganda M, Vorontsova MS, Hall R, Elia J, et al. 2015.** Photosynthetic innovation broadens the niche within a single species. *Ecology Letters* **18**(10): 1021-1029.
- Lundgren MR, Christin P-A, Gonzalez Escobar E, Ripley BS, Besnard G, Long CM, Hattersley PW, Ellis RP, Leegood RC, Osborne CP. 2016.** Evolutionary implications of C₃-C₄ intermediates in the grass *Alloteropsis semialata*. *Plant, Cell & Environment* DOI: [10.1111/pce.12665](https://doi.org/10.1111/pce.12665).
- Lundgren MR, Osborne CP, Christin P-A. 2014.** Deconstructing Kranz anatomy to understand C₄ evolution. *Journal of Experimental Botany* **65**(13): 3357-3369.
- Majeran W, van Wijk KJ. 2009.** Cell-type-specific differentiation of chloroplasts in C₄ plants. *Trends in Plant Science* **14**(2): 100-109.
- McQualter RB, Bellasio C, Gebbie L, Petrasovits LA, Palfreyman R, Hodson M, Plan M, Blackman D, Brumbley S, Nielsen L. 2016.** Systems biology and metabolic modelling unveils limitations to polyhydroxybutyrate accumulation in sugarcane leaves; lessons for C₄ engineering. *Plant Biotechnology Journal* **124**(2): 567–580.
- Mouliya B, Fournier M, Guitard D. 1994.** Mechanics and form of the maize leaf: in vivo qualification of flexural behaviour. *Journal of Materials Science* **29**(9): 2359-2366.
- Nakamura N, Iwano M, Havaux M, Yokota A, Munekage YN. 2013.** Promotion of cyclic electron transport around photosystem I during the evolution of NADP–malic enzyme-type C₄ photosynthesis in the genus *Flaveria*. *New Phytologist* **199**(3): 832-842.
- Niinemets Ü, Portsmuth A, Tobias M. 2007.** Leaf shape and venation pattern alter the support investments within leaf lamina in temperate species: a neglected source of leaf physiological differentiation? *Functional Ecology* **21**(1): 28-40.
- Osborne CP, Salomaa A, Kluyver TA, Visser V, Kellogg EA, Morrone O, Vorontsova MS, Clayton WD, Simpson DA. 2014.** A global database of C₄ photosynthesis in grasses. *New Phytologist* **204**(3): 441-446.
- Peng L, Yamamoto H, Shikanai T. 2011.** Structure and biogenesis of the chloroplast NAD(P)H dehydrogenase complex. *Biochimica et Biophysica Acta - Bioenergetics* **1807**(8): 945-953.
- Sack L, Scoffoni C. 2013.** Leaf venation: structure, function, development, evolution, ecology and applications in the past, present and future. *New Phytologist* **198**(4): 983-1000.
- Sage RF. 2004.** The evolution of C₄ photosynthesis. *New Phytologist* **161**(2): 341-370.
- Sage RF. 2014.** Stopping the leaks: New insights into C₄ photosynthesis at low light. *Plant, Cell & Environment* **37**(5): 1037-1041.
- Sage RF, Khoshravesh R, Sage TL. 2014.** From proto-Kranz to C₄ Kranz: building the bridge to C₄ photosynthesis. *Journal of Experimental Botany* **65**(13): 3341-3356.
- Schneider CA, Rasband WS, Eliceiri KW. 2012.** NIH Image to ImageJ: 25 years of image analysis. *Nature Methods* **9**(7): 671-675.
- Sheehy JE, ed. 2007.** Charting New Pathways to C₄ Rice. Los Baños, Philippines: International Rice Research Institute.
- Sun WEI, Ubierna N, Ma J-Y, Cousins AB. 2012.** The influence of light quality on C₄ photosynthesis under steady-state conditions in *Zea mays* and *Miscanthus × giganteus*: changes in rates of photosynthesis but not the efficiency of the CO₂ concentrating mechanism. *Plant, Cell & Environment* **35**(5): 982-993.
- Terashima I, Wong SC, Osmond CB, Farquhar GD. 1988.** Characterization of non-uniform photosynthesis induced by abscisic-acid in leaves having different mesophyll anatomies. *Plant and Cell Physiology* **29**(3): 385-394.
- Ubierna N, Sun W, Kramer DM, Cousins AB. 2013.** The efficiency of C₄ photosynthesis under low light conditions in *Zea mays*, *Miscanthus × giganteus* and *Flaveria bidentis*. *Plant, Cell & Environment* **36**: 365-381.
- Ueno O, Sentoku N. 2006.** Comparison of leaf structure and photosynthetic characteristics of C₃ and C₄ *Alloteropsis semialata* subspecies. *Plant Cell and Environment* **29**(2): 257-268.
- von Caemmerer S, Furbank RT. 2003.** The C₄ pathway: an efficient CO₂ pump. *Photosynthesis Research* **77**(2-3): 191-207.
- von Caemmerer S, Quick WP, Furbank RT. 2012.** The development of C₄ rice: current progress and future challenges. *Science* **336**(6089): 1671-1672.
- Yamori W, Shikanai T. 2016.** Physiological functions of cyclic electron transport around photosystem i in sustaining photosynthesis and plant growth. *Annual review of plant biology* **67**(1): 81-106.
- Yin X, Struik PC. 2015.** Constraints to the potential efficiency of converting solar radiation into phytoenergy in annual crops: from leaf biochemistry to canopy physiology and crop ecology. *Journal of Experimental Botany* **66**(21): 6535-6549.
- Yin X, Van Oijen M, Schapendonk A. 2004.** Extension of a biochemical model for the generalized stoichiometry of electron transport limited C₃ photosynthesis. *Plant, Cell & Environment* **27**(10): 1211-1222.
- Yin XY, Struik PC. 2012.** Mathematical review of the energy transduction stoichiometries of C₄ leaf photosynthesis under limiting light. *Plant Cell and Environment* **35**(7): 1299-1312.
- Yin XY, Sun ZP, Struik PC, Van der Putten PEL, Van Ieperen W, Harbinson J. 2011.** Using a biochemical C₄ photosynthesis model and combined gas exchange and chlorophyll fluorescence measurements to estimate bundle-sheath conductance of maize leaves differing in age and nitrogen content. *Plant Cell and Environment* **34**(12): 2183-2199.
- Zhong RQ, Taylor JJ, Ye ZH. 1997.** Disruption of interfascicular fiber differentiation in an *Arabidopsis* mutant. *Plant Cell* **9**(12): 2159-2170.

Figures.

Figure 1. From anatomy to light penetration. Panel **a** is an example of a C_4 *A. semialata* (MDG) leaf in cross-section, where the dashed lines show the region subject to anatomical measurements. Panel **b** schematises how anatomical characteristics were derived (results are reported in Table 2 and Supporting Information Table S2). Within one interveinal distance (IVD), the cross-sectional height along the vein, the abaxial and adaxial bundle sheath extensions (AD.BSE and AB.BSE) as well as vein height and width (with the term vein encompassing the vascular bundle, VB, and inner and outer bundle sheaths, IBS, and OBS) were measured. Panel **c** shows the modelled leaf anatomy. A rectangular vein is surrounded by three portions of mesophyll: interveinal M (MI), adaxial M (MAD), and abaxial M (MAB). The measured height at the vein is taken as $N=1000$ layers; the height of upper and lower BSE are taken as thicknesses of the MAD and MAB, respectively (expressed as n_{MAD} and n_{MAB}), while the vein equivalent height (VEH) is calculated as the difference (expressed as n_{VEIN} , where $N=n_{MAD}+n_{VEIN}+n_{MAB}$). Light penetration was modelled through profiles P1 (sectioning vertically through the interveinal M) and P2 (sectioning vertically through the vein) with an absorption and scattering model, and calibrated so that the overall leaf reflectance and transmittance is equal to 0.1. The presence of BSE was accounted for by diluting the pigmentation of MAD and MAB. Panel **d** shows profiles of light penetration in the leaf, calculated for the average anatomy across six accessions (Table 2) and with relative vein pigmentation $\frac{k_V}{k_{MI}}=1.5$. The downward photon flux I , as a fraction of incident photon flux I_0 (I/I_0 , dimensionless), is plotted against the depth in the absorbing path of the leaf, relative to N , for P1 (solid line) and P2 (dashed line). Note that P2 is less steep than P1 in correspondence of MAD, which is paler than interveinal M for the presence of BSE ($\frac{k_{MA}}{k_{MI}} < 1$), while P2 is steeper than P1 in correspondence of the vein, which is darker than interveinal M ($\frac{k_{VB}}{k_{MI}} > 1$).

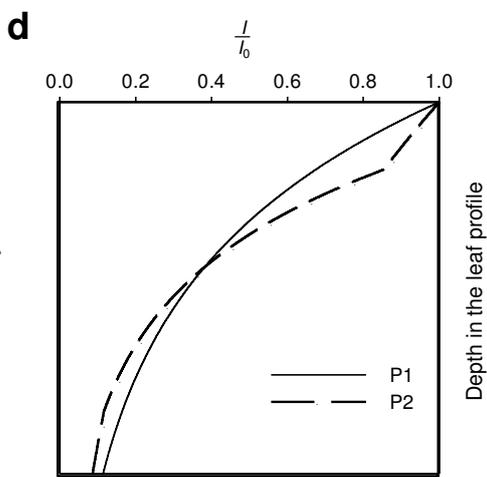
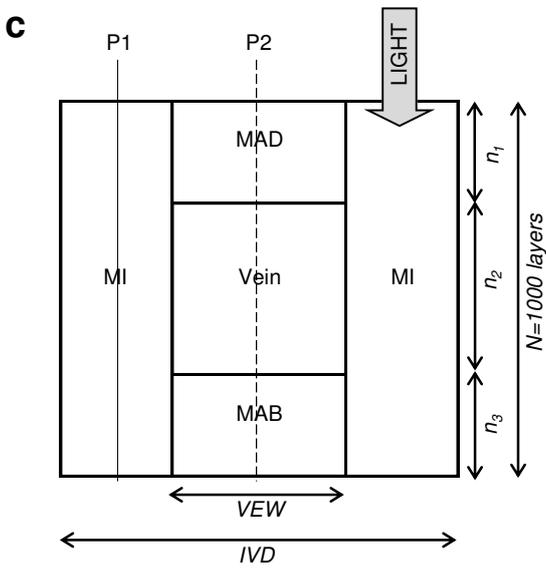
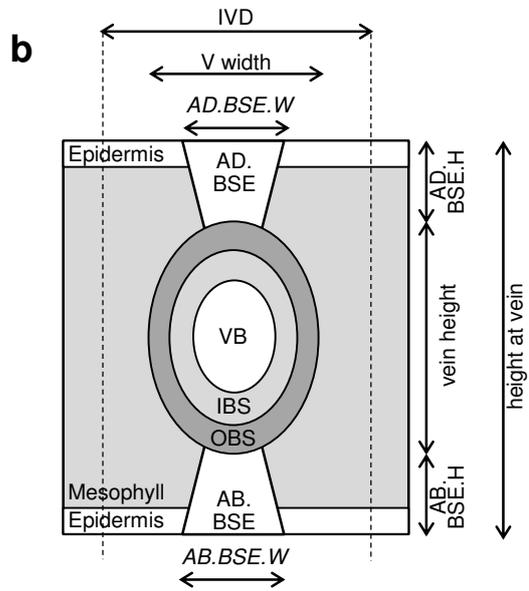
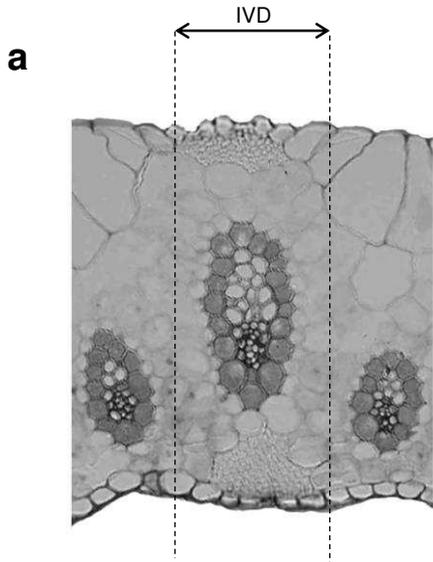


Figure 2. Model simulations. To show the possible anatomical constraints to light harvesting and ATP production in the BS, the operational conditions typical of each photosynthetic type (Table 2) are selectively manipulated. Panel **a** shows the potential for light harvesting in the BS ($AB \frac{BS}{M}$), along different relative vein pigmentations ($\frac{k_V}{k_{MI}}$) for the anatomical types listed in Table 2. The operational vein pigmentation $\frac{k_V}{k_{MI}}$, experimentally estimated as the apparent relative absorbance (ARA, Table 2), are marked with asterisks. Panel **b** shows the possible trade-offs between vein pigmentation ($\frac{k_V}{k_{MI}}$) and vein size ($\frac{VEW}{IVD}$) required for a light absorption target ($AB \frac{BS}{M}$). Panel **c** shows the effect of bundle sheath extensions (BSE) on BS light absorption ($AB \frac{BS}{M}$), simulated by changing BSE shading ($\frac{k_{MA}}{k_{MI}}$), at different levels of vein pigmentations ($\frac{k_V}{k_{MI}}$). Panel **d** shows the effect of manipulating $rAB_{CEF\ BS}$, the fraction of absorbed light used by cyclic electron flow, on relative ATP production in BS ($\frac{J_{ATP\ BS}}{J_{ATP\ M}}$, Eqn 2), calculated for a hypothetical vein pigmentation equivalent to that of interveinal M ($\frac{k_V}{k_{MI}} = 1$). The bold line represents the minimum threshold for regenerating RuBP in BS ($\frac{J_{ATP\ BS}}{J_{ATP\ M}} = 0.3$) (Bellasio & Griffiths, 2014c). The *A. semialata* accessions KWT and L01 are not shown for simplicity, however, values are reported in Table 2 and Supporting Information Table S2.

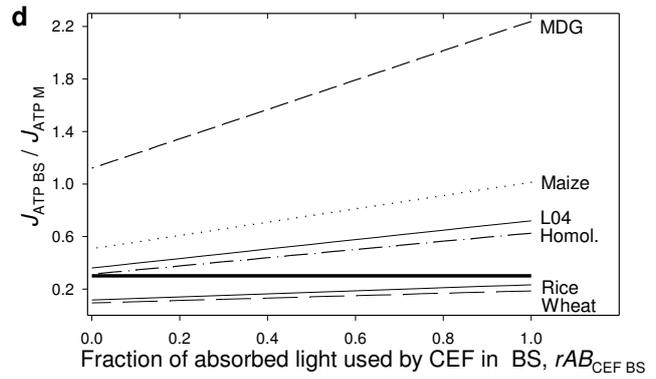
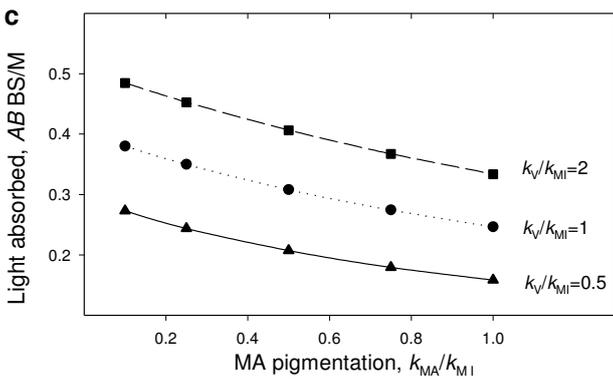
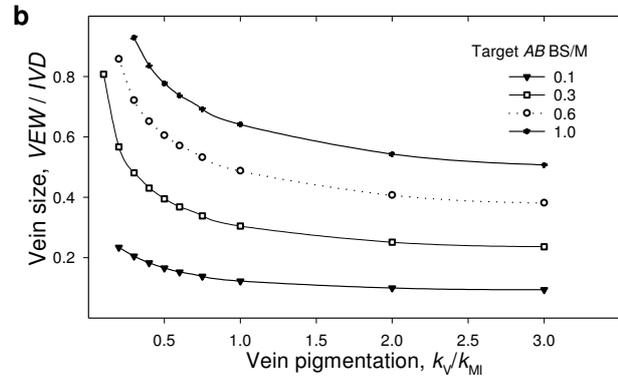
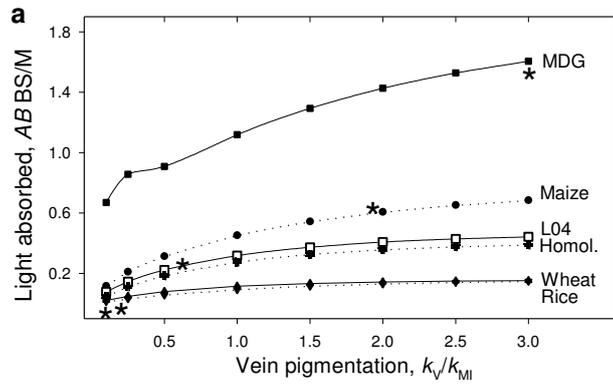


Figure 3. Trade-off between vein size and vein pigmentation. The experimental range of pigmentation and size across the evolutionary continuum between C_3 and C_4 is shown by squares (from left to right rice, wheat, KWT3, L04D, L01A, maize and MDG1, values are reported in Table 2 and Supporting Information Table S2). The line r is the line of best fit ($R^2=0.98$) representing all optimal resource combination for the measured accessions.

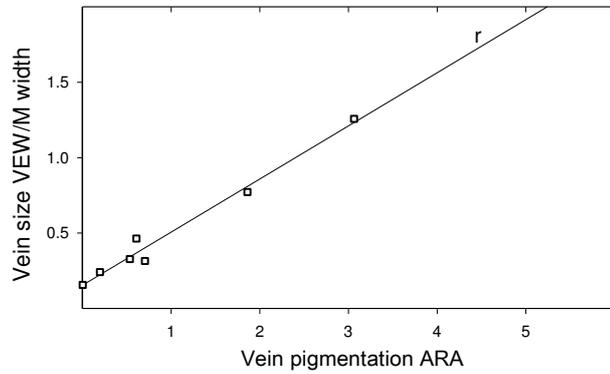
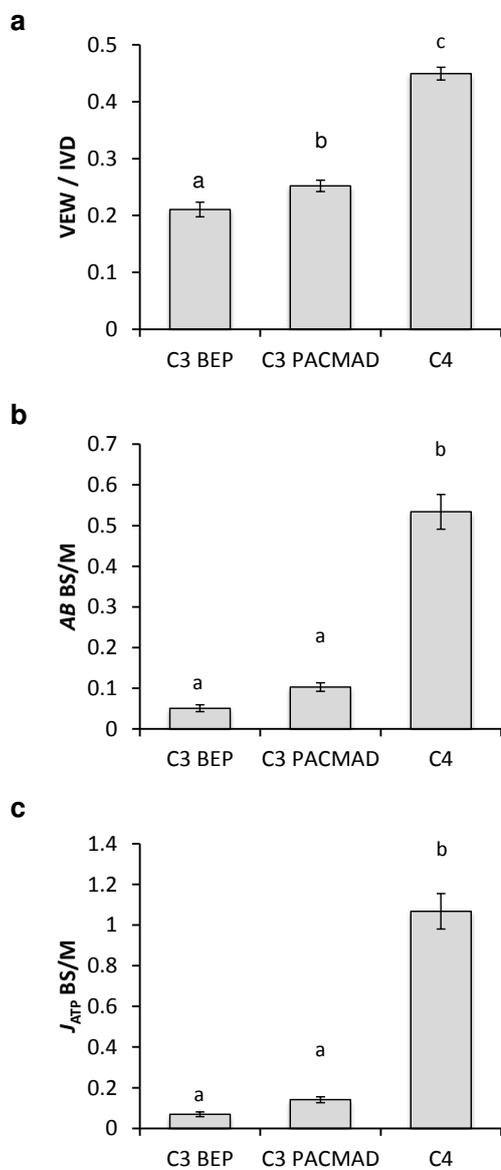


Figure 4. Light harvesting across the grass phylogeny. From the anatomical characteristics of 145 species (Christin et al., 2013), we derived the key inputs VEW/IVD shown in panel **a**. Potentials for light harvesting in the BS ($AB \frac{BS}{M}$, panel **b**) was calculated using values for ARA estimated from the linear regression shown in Fig. 3, through a routine detailed in Supporting Information File S1, Note 2. Leaf reflectance and transmittance were fitted to values typical of penetrating radiation, thus the values of $AB \frac{BS}{M}$ that we show represent the theoretical maximum achieved under optimal BS illumination. The relative ATP production in the BS ($\frac{J_{ATP BS}}{J_{ATP M}}$) shown in panel **c** was calculated using likely values for $rAB_{CEF BS}$ (Table 2). Mean \pm SE. C₃ BEP, n=34; C₃ PACMAD, n= 61; C₄, n= 50. Values labelled with different letters were deemed significant at $p < 0.05$ in Tukey post-hoc tests.



Tables.

Table 1. Acronyms, variables, and units used.

Symbol	Definition	Unit
<i>AB</i>	Absorbed light as a fraction of incident light	dimensionless
<i>AD.BSE.H</i> , <i>AB.BSE.H</i>	Height of adaxial and abaxial BSE, respectively	μm
<i>AD.BSE.W</i> , <i>AB.BSE.W</i>	Width of adaxial and abaxial BSE, respectively	μm
ARA	Apparent relative absorbance, Eqn 1, Experimental proxy for vein pigmentation $\frac{k_V}{k_{MI}}$	dimensionless
BS	Bundle sheath	
BSE	Bundle sheath extension and extraxylary fibres, collectively	
CCM	Carbon concentrating mechanism	
CEF	Cyclic electron flow	
<i>I</i> , <i>I₀</i>	Downward photon flux, Incident photon flux	arbitrary
IBS	Inner bundle sheath	
IVD	Interveinal distance	μm
<i>J</i>	Upward photon flux	arbitrary
<i>J_{ATP}</i> , <i>J_{ATP BS}</i> , <i>J_{ATP M}</i>	ATP production rate, unspecified, in BS or in M respectively	μmol m ⁻² s ⁻¹
<i>k</i> , <i>k_V</i> , <i>k_{MI}</i> , <i>k_{MA}</i>	Absorption parameter, representing the density of light harvesting machinery, unspecified, in vein, interveinal M, and collectively abaxial and abaxial mesophyll, respectively	dimensionless
LEF	Linear electron flow	
η , η_{LEF} , η_{CEF}	Overall conversion efficiency of AB in ATP, general, of LEF and CEF, respectively	
$\Gamma_{AB_{CEF BS}}$	Proportion of <i>AB_{BS}</i> used by CEF	
<i>M</i> , <i>MI</i> , <i>MAD</i> , <i>MAB</i> , <i>MA</i>	Mesophyll, unspecified, interveinal, adaxial, abaxial or collectively adaxial and abaxial, respectively	
<i>N</i> , <i>n</i> , <i>n_{MAD}</i> , <i>n_{VEIN}</i> , <i>n_{MAB}</i>	Total layers (1000) in which the light absorbing portion of the leaf is divided, a generic layer, number of layers assigned to MAD, number of layers assigned to the vein, number of layers assigned to MAB, respectively	
OBS	Outer bundle sheath	
P1	Plot of light intensity <i>versus</i> depth (light profile) in correspondence of interveinal M	
P2	Plot of light intensity <i>versus</i> depth (light profile) in correspondence of the vein	
<i>R</i> , <i>R_g</i> , <i>R_{LEAF}</i>	Reflectance, unspecified, of the last layer, and of the leaf respectively	0.06
<i>RPP</i>	Reductive pentose phosphate (cycle); also known as Calvin–Benson–Bassham cycle or photosynthetic carbon reduction cycle	
RuBP	Ribulose-1,5-bisphosphate	
<i>VEH</i>	Vein equivalent height $VEH = height\ at\ vein - AD.BSE.H - AB.BSE.H$	μm
<i>VEW</i>	Vein equivalent width $VEW = \frac{VB\ Area}{VEH}$	μm
WAV	Weighted average RGB histogram value, or luminosity	

Table 2. Operational conditions in the C₃ to C₄ anatomical continuum. Basic anatomical characteristics, inputs to the optical model (next to the underpinning measured quantity, in parentheses), and model output obtained for eight accessions. The complete dataset is included in Supporting Information Table S2. Species marked with an asterisk are averaged in the last column.

	rice*	wheat*	<i>A. semialata</i> KWT	<i>H. aturensis</i> *	<i>A. semialata</i> L01	<i>A. semialata</i> L04*	maize*	<i>A. semialata</i> MDG*	Average (of 6 accessions with *)
Photosynthetic type	C ₃	C ₃	C ₃	C ₃ -C ₄	C ₃ -C ₄	C ₃ -C ₄	C ₄	C ₄	-
Anatomical characteristics									
Height at vein / μm	83.5	174	207	95.4	150	209	152	225	164
<i>IVD</i> / μm	273	313	255	207	195	195	124	85.5	200
Vein area / μm^2	2228	5306	6614	4744	5330	9338	4970	7900	5747
Input									
η_{MAD}	179	249	244	138	69	148	218	83	169
η_{VEIN}	727	502	510	761	764	725	605	739	676
η_{MAB}	94	249	246	101	167	127	178	178	154
<i>VEW</i> / <i>IVD</i>	0.134	0.194	0.246	0.316	0.239	0.316	0.436	0.557	0.325
$\frac{k_{\text{MA}}}{k_{\text{MI}}}$ (MA pigmentation)	0.292	1	0.296	0.637	0.207	0.211	0.211	0	0.392
<i>ARA</i> (relative vein pigmentation, $\frac{k_{\text{V}}}{k_{\text{MI}}}$)	0.0033	0.198	0.535	-	0.705	0.609	1.86	3.06	1.28
<i>rAB</i> _{CEF BS}	0.375	0.375	0.375	0.7	0.7	0.7	1	1	0.7
Output									
$AB \frac{\text{BS}}{\text{M}}$	0.001	0.026	0.129	-	0.23	0.284	0.66	1.606	0.363
$\frac{J_{\text{ATP BS}}}{J_{\text{ATP M}}}$	0.001	0.036	0.177	-	0.391	0.483	1.32	3.21	0.617